IOP Publishing Physica Scripta
Phys. Scr. 95 (2020) 045701 (11pp) https://doi.org/10.1088/1402-4896/ab57cf

Improving the efficiency of gas turbine-air bottoming combined cycle by heat exchangers and bypass control valves

M N Khan[1], M Osman[1,2], Abdulaziz R Alharbi[3], Mohammad Rahimi Gorji[4] and Ibrahim M Alarifi[1,5]

[1] Department of Mechanical and Industrial Engineering, College of Engineering, Majmaah University, Majmaah 11952, Saudi Arabia
[2] Department of Mechanical Design, Faculty of Engineering Mataria, Helwan University, Cairo, Egypt
[3] Department of mechanical engineering, Fahad Bin Sultan University, Tabuk, 71454 Saudi Arabia
[4] Faculty of Medicine and Health Science, Ghent University, Gent B-9000, Belgium

E-mail: mohammad.rahimigorji@ugent.be, m69.rahimi@yahoo.com and i.alarifi@mu.edu.sa

Received 12 August 2019, revised 22 October 2019
Accepted for publication 14 November 2019
Published 11 February 2020

Abstract

The present study is a comparative energy and exergy analysis of a Proposed gas turbine cycle (PGTC) with a simple gas turbine cycle (SGTC), maintaining the same rate of fuel supply in both cycles. In the PGTC, the air bottoming cycle is operated by exhaust gases from the topping gas turbine cycle by exchanging heat in the heat exchangers (H.E.s) by controlling the path of exhaust gases and compressed air through the bypass control valves. The bypass valve in the topping, as well as the bottoming cycle, direct the combustible product from the combustion chamber to the H.E., in such a way that it optimizes the performance of the proposed combined cycle as compared to SGTC. The results show that the maximum increase in Work net output and thermal efficiency in PGTC compared to SGTC is 65.7% at $r_p = 4$ and turbine inlet temperature (TIT) = 1500 K, whereas the exergy loss by the exhaust gases in the PGTC is much less than the exergy loss by the exhaust gases in the SGTC. The maximum difference in the exergy loss by the exhaust gases in PGTC and SGTC is also observed at $r_p = 4$ and TIT = 1500 K.

Keywords: gas turbine, turbine inlet temperature, heat exchanger, bypass valve, exergy loss, exergetic efficiency

(Some figures may appear in colour only in the online journal)

Nomenclature

W_{net}	work net output
$\dot{Q}$	rate of heat supplied
ε	heat exchanger effectiveness
η	efficiency
$\dot{m}$	mass flow rate
r_p	pressure ratio
T	temperature (K)
SGTC	simple gas turbine cycle
c_p	specific heat
γ	specific heat ratio
H.E.	heat exchanger
SFC	specific fuel consumption
E	exergy
LCV	lower calorific value of fuel
TIT	turbine inlet temperature

[5] Author to whom any correspondence should be addressed.

PGTC	proposed gas turbine cycle

Subscripts

c	compressor
T	turbine
cc	combustion chamber
s	simple gas turbine cycle
net	net
a	air
Th	thermal
t	topping-cycle
b	bottoming cycle
Comb	combined
f	fuel
g	gas
Exh	exhaust

1. Introduction

The environmental impact of the gas turbine has been considered in this current research by increasing the total exergy loss using a novel model. The energy and exergy are important indicators for evaluating the gas turbine's performance, especially for environmental control and safe gas combustion. One of the main motivations behind this research is to position the bypass valves (BPV) and H.E.s in a gas turbine-air bottoming combine cycle in such a way that not only reduces the exergy loss from the exhaust gases of the gas turbine to the maximum extent but also enhances the cycle's performance, as compared to the results available in the literature.

Najafi *et al* [1] observed that for the optimization technique, the optimal solutions set and the final designated optimal design, achieved an exergetic efficiency of 46%, from a total cost of 3.76 million USD annually. The results indicate that for multi-objective optimization, besides preserving high exergetic efficiency, the total system cost is also reduced [1]. In another comparative study in the literature, the results revealed that conventional combined cycles could reach the highest thermal efficiency of about 48%, especially when the topping gas turbine and bottoming steam turbine cycles are thermodynamically efficient [2]. Moon *et al* achieved coolant intercooling, which was implemented to decrease the coolant temperature and enhance the gas turbine's performance [3]. The component model contains more details, such as a compressor, turbine model with a cooling system for evaluating the usefulness of the compressor, and turbine regulations [4, 5].

In another studies, it was observed that the variation in the bottoming cycle depended on the effective energy utilization possible in the topping cycle. Also, the authors found the bottoming cycle uses a steam cycle or ammonia water cycle, or a mixture, and their scope of work suggests further improvement in the combined cycle performance is possible [6–8]. The performance of the gas turbine was analyzed, including the resulting inlet and outlet cooling stages, and the gas turbine's performance showed that it produced the largest turbine efficiency [9]. The gas turbine power plant energy and exergy analysis were conducted based on the combustion chamber, which showed the most exergy destruction in the system due to high irreversibility during the combustion process [10, 11]. Besides, simulations of fixed parameters showed that humidifying the air has a substantial impact on cycle performance due to the improved heat recovery from waste and other types of heat [12, 13].

In another study, the gas turbine energy exhaust was recovered through a pre-heating water process and then adding water before the combustor, leading to high overall thermal efficiency. Kumari and Sanjay [14] observed that the intercool gas turbine delivered higher gas turbine results and higher thermal efficiency compared with the basic design of the gas turbine. The pressure ratio of the intercool gas turbine has a higher enhanced power output compared to a typical gas turbine, and the exergy results revealed a higher ratio and efficiency from a combustion turbine [15].

Selwynraj *et al* [16] evaluated both a gas turbine and steam turbine, in particular, the exergetic efficiency and exergy magnitude increased by about 5%, and the condenser air cooling ensured that the last portion of exergy in the gas turbine system was removed. In that study, the exhaust system of the gas turbine reduced the exergy losses, and the efficiency observed was about 58%, and this increased when the steam injection was applied [17]. The performance and design thermodynamic in power plant are assessment energy and exergy analysis after modification of the combustion chamber the exergy range has been improved [18]. The exergy loss and exergetic enhancement have been considered in several studies, then these studies compare the basic model of the gas turbine suggest the new design based on the calculation of both exergy efficiencies were analyzed [19–22]. Environmental issues and saving energy and exergy are important when considering saving energy and the improvement of gas turbine efficiency; especially, this technology is increasing in the drive to achieve better and more efficient gas turbine power plants [23, 24]. The gas turbine combine cycle included the bottom stream turbine and a topping gas turbine cycle are the most measurable efficiency for the gas turbine in using energy and exergy analysis with combine preheating and cooling in the power plant system [25–28]. The exhaust turbine of a topping cycle was used to run the air bottoming cycle, and the major parameters affecting the performance of the combined air bottoming cycle were found to be pressure ratio, TIT and the inlet temperature of the air [28–33]; whereas the other parameters affecting the combined cycle performance, especially the air bottoming cycle, are the effectiveness of the H.E. and the right path for the exhaust gases to exchange maximum heat for the topping as well as bottoming cycle [34, 35].

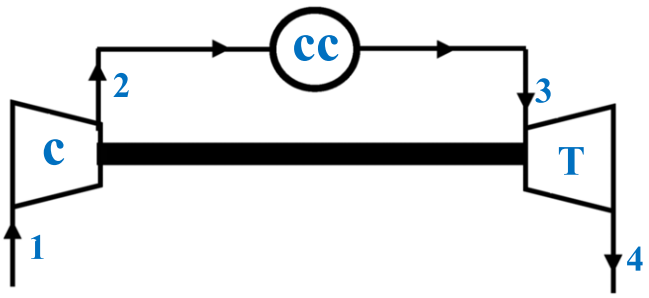

Figure 1. Schematic diagram of a simple gas turbine cycle (SGTC).

The concept of H.E. in a simple gas turbine is first briefly discussed by Hernandez *et al* [36] in 1995 as a regenerative gas turbine cycle, and after that, several researchers did many modifications in the regenerative air standard cycles to enhance cycle performance [37–42]. When the temperature of compressed air from the air compressor becomes more than the exhaust gases, in SGTC or combined air bottoming cycle, the heat is transfer from the compressed air to the exhaust gases that result in a decrease in cycle efficiency as well as an increase in exergy loss by exhaust gases. Khan *et al* [43, 44] proposed the concept of BPV with a H.E. which helps to further increase in cycle efficiency and decrease in exergy loss by exhaust gases. This implies that the concept of the H.E. as well as BPV in a SGTC and combined air bottoming cycle is not new. The positioning of the H.E. and BPV in the combined air bottoming cycle is very important to enhance the cycle performance. The novelty of the present study is the combination of H.E.s and BPV which direct the combustible product through the H.E.s in such a way that not only enhances work net output and overall thermal efficiency of the PGTC which results in minimizing the cost of power generation but also minimize the exergy losses by the exhaust gases which contribute in controlling the problem of global warming.

The major difficulty and challenge to achieving the results lie in developing a mathematical model for the PGTC, and the second most difficult aspect of this study is to write the program of the mathematical model developed in an engineering equation solver (EES) program because it requires many logical functions.

2. Cycle description

2.1. Cycle description of SGTC

Figure 1 shows a schematic diagram of the SGTC in which air is at ambient temperature T_1, and pressure P_1 enters the air compressor where its pressure and temperature rise to P_2 and T_2 respectively. The compressed air leaving the air compressor enters the combustion chamber, where its temperature further increases from T_2 to T_3. The combustible product from the combustion chamber at pressure P_2 and temperature T_3(TIT) enters the gas turbine where it expands to the pressure of P_4 and temperature T_4.

2.2. Cycle analysis

Power required to run the air compressor

$$(W_c) = \dot{m}_a.c_{pa}.T_1.\left(\frac{r_p^k - 1}{\eta_c}\right), \tag{1}$$

where $k = (\gamma - 1)/\gamma$.

Temperature of air at the exit of the air compressor

$$(T_2) = T_1.\left\{1 + \frac{r_p^k - 1}{\eta_c}\right\}. \tag{2}$$

Mass flow rate of fuel

$$(\dot{m}_f)_s = \dot{m}_a.\left\{\frac{c_{pg}.\mathrm{TIT} - c_{pa}.T_2}{cv - c_{pg}.\mathrm{TIT}}\right\}. \tag{3}$$

Mass flow rate of combustible gases from the combustion chamber

$$(\dot{m}_g)_s = \dot{m}_a.\left\{\frac{cv - c_{pa}.T_2}{cv - c_{pg}.\mathrm{TIT}}\right\}. \tag{4}$$

Temperature of gases at the exit of the gas turbine

$$(T_4) = \mathrm{TIT}.\{1 - \eta_T.(1 - r_p^{-k'})\}, \tag{5}$$

where $k' = (\gamma' - 1)/\gamma'$.

Power delivered by the gas turbine

$$(W_T)_s = (\dot{m}_g)_s.c_{pg}.\mathrm{TIT}.\eta_T(1 - r_p^{-k'}). \tag{6}$$

Work net output of the cycle

$$(W_{\mathrm{net}})_s = W_T - W_c. \tag{7}$$

Rate of heat supplied by the combustion chamber

$$(\dot{Q})_s = (\dot{m}_g)_s.c_{pg}.\mathrm{TIT} - \dot{m}_a.c_{pa}.T_2. \tag{8}$$

Thermal efficiency

$$(\eta_{\mathrm{th}})_s = \frac{(W_{\mathrm{net}})_s}{(\dot{Q})_s} \times 100. \tag{9}$$

SFC

$$(\mathrm{SFC})_s = 3600.\frac{(\dot{m}_f)_s}{(W_{\mathrm{net}})_s}. \tag{10}$$

Exergy destruction of compressor due to irreversibility

$$(E_c) = \dot{m}_a.T_0.(s_2 - s_1) = \dot{m}_a.T_0.\left\{c_{pa}.\ln\left(\frac{T_2}{T_1}\right) - R_a.\ln(r_p)\right\}. \tag{11}$$

Exergy destruction of combustion chamber due to irreversibility

$$(E_{cc})_s = T_0.\left[\dot{m}_g.\left\{c_{pg}.\ln\left(\frac{T_3}{T_0}\right) - R_g.\ln\left(\frac{P_3}{P_0}\right)\right\} - \dot{m}_a.\left\{c_{pa}.\ln\left(\frac{T_2}{T_0}\right) - R_a.\ln\left(\frac{P_2}{P_0}\right)\right\}\right] + (\psi - 1).\dot{m}_f.(\mathrm{LCV})_{T_0}. \tag{12}$$

Bypass Valve Open : This means that gases/air Bypass the Heat Exchanger
Bypass Valve Close : This means that gases/air pass through the Heat Exchanger

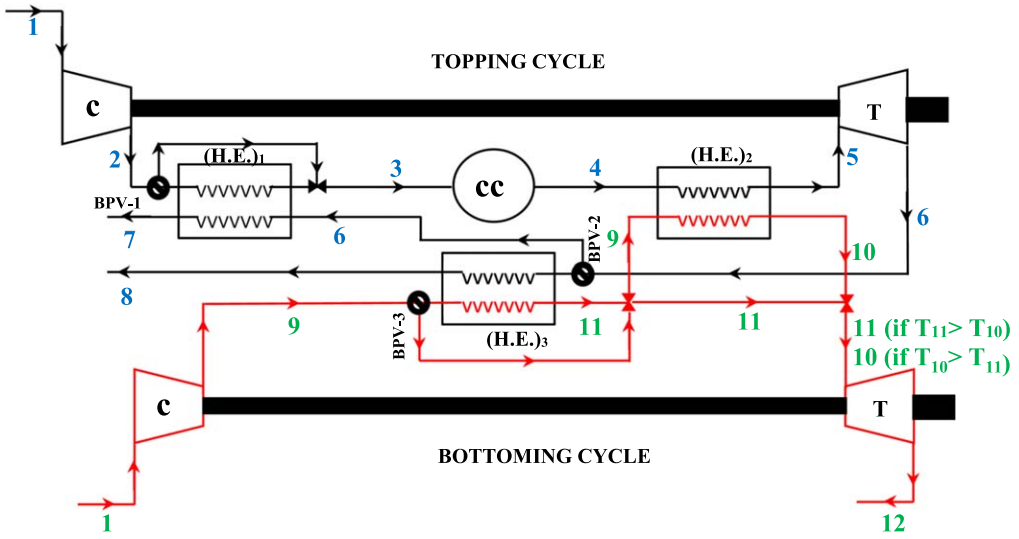

Figure 2. Schematic diagram of the proposed air bottoming combined cycle (PABCC).

Exergy destruction of gas turbine due to irreversibility

$$(E_T)_s = \dot{m}_g.T_0.\,(s_4 - s_3) = \dot{m}_g.T_0.\left\{c_{pg}.\ln\left(\frac{T_4}{T_3}\right) - R_g.\ln\left(\frac{1}{r_p}\right)\right\}. \quad (13)$$

Exergy lost due to exhaust flue gas

$$(E_{\mathrm{Exh}})_s = \int_{T_0}^{T_4}\left(1 - \frac{T_0}{T}\right).\mathrm{d}Q = \dot{m}_g.c_{pg}.\left\{(T_4 - T_0) - T_0.\ln\left(\frac{T_4}{T_0}\right)\right\}. \quad (14)$$

Total exergy lost due to irreversibility

$$(E_{\mathrm{total}})_s = \sum_{1}^{n}(E_n). \quad (15)$$

Exergetic efficiency

$$(\eta_E)_s = \left(\frac{(W_{\mathrm{net}})_s}{(E_{\mathrm{total}})_s + (W_{\mathrm{net}})_s}\right) \times 100. \quad (16)$$

2.3. Cycle description of the PGTC

Figure 2 shows the schematic diagram of the PGTC in which air at ambient temperature T_1 and pressure P_1 enters the air compressor, where the pressure and temperature raise to P_2 and T_2 respectively. The compressed air from the air compressor enters the combustion chamber via the first heat exchanger $(\mathrm{H.E.})_1$ if the temperature of exhaust gases of the gas turbine is more than the temperature of compressed air from the air compressor, and under this condition bypass valve 1 (BPV-1) is closed and bypass valve 2 (BPV-2) is open due to which the temperature of compressed air rises from T_2 to T_3, given by the equation (18). But if the temperature of the exhaust gases is less than the temperature of compressed air from the air compressor of topping cycle, then the; then the compressed air from the air compressor directly enters the combustion chamber without passing through the $(\mathrm{H.E.})_1$, and under such condition BPV-1 is open and BPV-2 is close. The temperature of the combustible product leaving the combustion chamber is given by equation (20), which is more than the TIT of the SGTC, because of the same rate of fuel supply in both cycles, and the inlet temperature of the air to the combustion chamber in the PGTC is more than the inlet temperature of the air to the combustion chamber in SGTC. In PGTC, the combustible product enters the gas turbine of the topping cycle via a second heat exchanger $(\mathrm{H.E.})_2$, and the combustible product exchanges heat with the compressed air of the bottoming cycle if the bypass valve 3 (BPV-3) is open. The combustible product exchanges heat with the compressed air of the bottoming cycle, such that the temperature of the combustible product entering the topping gas turbine of the PGTC is the same as the temperature of the combustible product in the SGTC.

Also if the temperature of exhaust gases is less than the temperature of compressed air from the air compressor of the topping cycle, at this stage the temperature of the combustible product leaving the combustion chamber becomes the same in both the PGTC and the SGTC. And at this stage the BPV-1 is open, the BPV-2 is close, and the BPV-3 is close. This allows compressed air from the air compressor of the bottoming cycle, and exhaust gases of the topping cycle passes through the $(\mathrm{H.E.})_3$, and this results in raises in temperature of compressed air of bottoming cycle from T_9 to T_{11} and drop in temperature of exhaust gasses from T_6 to T_8.

2.4. Analysis of the PGTC

2.4.1. Analysis of topping cycle. Power required to run the air compressor of the topping cycle

$$(W_c)_t = \dot{m}_{at}.c_{pa}.T_1.\left(\frac{r_{pt}^k - 1}{\eta_c}\right), \tag{17}$$

where

$$(T_2) = T_1.\left\{1 + \frac{r_p^k - 1}{\eta_c}\right\};$$

$r_{pt} = r_p$(Pressure Ratio of SGTC) and

$k = (\gamma - 1)/\gamma$.

The temperature of the air after leaving the $(\text{H.E.})_1$

$$T_3 = (1 - \varepsilon_1).T_2 + \varepsilon_1.\frac{(c_p)_{\max(T_6,T_2)}}{c_{pa}}.\ \text{Max}(T_6,\ T_2). \tag{18}$$

The temperature of exhaust gases after leaving the $(\text{H.E.})_1$

$$T_7 = T_6 - \left(\frac{1}{\varepsilon_1}\right).\left(\frac{c_{pa}}{c_{pg}}\right).\left(\frac{\dot{m}_a}{\dot{m}_g}\right).(\text{Max}\ .(T_2,\ T_3) - T_2). \tag{19}$$

The temperature of the combustible product after leaving the combustion chamber

$$T_4 = \frac{cv.(\dot{m}_f)_s + (\dot{m}_a)_s.c_{pa}.\ \text{Max}(T_3,\ T_2)}{(\dot{m}_g)_s.c_{pg}}. \tag{20}$$

The temperature of the combustible product after leaving the $(\text{H.E.})_2$

$$T_5 = \text{TIT}. \tag{21}$$

The temperature of the combustible product or exhaust gases at the exit of the gas turbine for the topping cycle

$$T_6 = \text{TIT}.\{1 - \eta_T.(1 - r_{pt}^{-k'})\}, \text{ where } k' = (\gamma' - 1)/\gamma'. \tag{22}$$

The temperature of exhaust gases after leaving the third Heat Exchanger $(\text{H.E.})_3$

$$T_8 = T_6 - \left(\frac{1}{\varepsilon_3}\right).\left(\frac{c_{pa}}{c_{pg}}\right).\left(\frac{(\dot{m}_a)_b}{(\dot{m}_g)_s}\right)(T_{11} - T_9). \tag{23}$$

The power delivered by the gas turbine from the topping cycle

$$(W_T)_t = \dot{m}_g.c_{pg}.\text{TIT}.\eta_T(1 - r_p^{-k'}). \tag{24}$$

Work net output of the cycle

$$(W_{\text{net}})_t = (W_T)_t - (W_c)_t. \tag{25}$$

The rate of heat supplied by the combustion chamber

$$(\dot{Q})_t = (\dot{m}_g)_s.c_{pg}.T_4 - (\dot{m}_a)_t.c_{pa}.\ \text{Max}(T_2,\ T_3). \tag{26}$$

2.4.2. Analysis of bottoming cycle. The temperature of air leaving the air compressor from the bottoming cycle

$$(T_9) = T_1.\left(1 + \frac{r_{pb}^k - 1}{\eta_c}\right), \tag{27}$$

where

$$r_{pb} = (x)^{\frac{1}{k+k'}} \tag{28}$$

And

$$x = \left(\frac{(\dot{m}_g)_s.c_{pg}.k'.\eta_c.\eta_t.}{(\dot{m}_a)_b.c_{pa}.k.T_1}\right).\ \text{Max}(T_{10},\ T_{11}). \tag{29}$$

Temperature of air leaving the $(\text{H.E.})_2$ of the bottoming cycle

$$T_{10} = T_9 + \varepsilon_2.\left(\frac{(\dot{m}_g)_s}{(\dot{m}_a)_b}\right).\left(\frac{c_{pg}}{c_{pa}}\right).(T_4 - \text{TIT}). \tag{30}$$

Temperature of air leaving the $(\text{H.E.})_3$ of the bottoming cycle

$$T_{11} = (1 - \varepsilon_3).T_9 + \varepsilon_3.\left(\frac{c_{pg}}{c_{pa}}\right).T_6 \text{ where if } T_2 > T_3. \tag{31}$$

Power required to run the air compressor for the bottoming cycle

$$(W_c)_b = (\dot{m}_a)_b.c_{pa}.T_1.\left(\frac{r_{pb}^k - 1}{\eta_c}\right). \tag{32}$$

Power delivered by the gas turbine for the bottoming cycle

$$(W_T)_b = (\dot{m}_a)_b.c_{pa}.\ \text{Max}(T_{11},\ T_{10}).\eta_T(1 - r_{pb}^{-k}). \tag{33}$$

Work net output of the bottoming cycle

$$(W_{\text{net}})_b = (W_T)_b - (W_c)_b. \tag{34}$$

2.4.3. Analysis of bottoming cycle. Work net output of the combined cycle

$$(W_{\text{net}})_{\text{comb}} = (W_{\text{net}})_t + (W_{\text{net}})_b. \tag{35}$$

Thermal efficiency

$$(\eta_{\text{th}})_{\text{comb}} = \frac{(W_{\text{net}})_{\text{comb}}}{(\dot{Q})_t} \times 100. \tag{36}$$

SFC

$$(\text{SFC})_{\text{comb}} = 3600.\frac{(\dot{m}_f)_s}{(W_{\text{net}})_{\text{comb}}}. \tag{37}$$

Total exergy destruction of compressor due to irreversibility

$$(E_c)_{\text{comb}} = (E_c)_t + (E_c)_b = (\dot{m}_a)_t.T_0.\left\{c_{pa}.\ln\left(\frac{T_2}{T_1}\right) - R_a.\ln(r_{pt})\right\} + (\dot{m}_a)_b.T_0.\left\{c_{pa}.\ln\left(\frac{T_9}{T_1}\right) - R_a.\ln(r_{pb})\right\}. \tag{38}$$

Exergy destruction of combustion chamber due to irreversibility

$$(E_{cc})_{\text{comb}} = T_0.\left[(\dot{m}_g)_s.\left\{c_{pg}.\ln\left(\frac{T_4}{T_0}\right) - R_g.\ln\left(\frac{P_4}{P_0}\right)\right\} - (\dot{m}_a)_t.\left\{c_{pa}.\ln\left(\frac{\text{Max}(T_2,\ T_3)}{T_0}\right) - R_a.\ln\left(\frac{P_2}{P_0}\right)\right\}\right] + (\psi - 1).(\dot{m}_f)_s.(\text{LCV})_0. \tag{39}$$

Total exergy destruction of the gas turbine due to irreversibility

$$(E_T)_{\text{comb}} = (E_T)_t + (E_T)_b = (\dot{m}_g)_s.T_0.\left\{c_{pg}.\ln\left(\frac{T_6}{T_5}\right) - R_g.\ln\left(\frac{1}{r_{pt}}\right)\right\} + (\dot{m}_a)_b.T_0.\left\{c_{pa}.\ln\left(\frac{T_{12}}{\text{Max}(T_{10},\ T_{11})}\right) - R_a.\ln\left(\frac{1}{r_{pb}}\right)\right\}. \tag{40}$$

Total exergy destruction of H.E. due to irreversibility

$$(I_{\text{H.E.}})_{\text{comb}} = (I_{\text{H.E}_1}) + (I_{\text{H.E}_2}) + (I_{\text{H.E}_3}), \tag{41}$$

where

$$(I_{H.E_1}) = (\dot{m}_a)_t.c_{pa}\left[(Max.(T_2,\ T_3) - T_2) - T_0.\ln\left(\frac{Max.(T_2,\ T_3)}{T_2}\right)\right] + (\dot{m}_g)_s.c_{pg}\left[(T_6 - T_7) - T_0.\ln\left(\frac{T_6}{T_7}\right)\right]$$

$$(I_{\text{H.E}_2}) = (\dot{m}_g)_s.c_{pg}[(\text{Max.}(\text{TIT},\ T_4) - \text{TIT}) - T_0.\ln\left(\frac{(\text{Max.}(\text{TIT},\ T_4) - \text{TIT})}{T_4}\right)\Bigg] + (\dot{m}_a)_b.c_{pg}\left[(T_{10} - T_9) - T_0.\ln\left(\frac{T_{10}}{T_9}\right)\right]$$

$$(I_{\text{H.E}_3}) = (\dot{m}_g)_s.c_{pg}\left[(T_6 - T_8) - T_0.\ln\left(\frac{T_6}{T_8}\right)\right] + (\dot{m}_a)_b.c_{pg}\left[(T_{11} - T_9) - T_0.\ln\left(\frac{T_{11}}{T_9}\right)\right]$$

if $T_3 \leqslant T_2$ and $T_4 \leqslant \text{TIT}$.

Exergy lost due to exhaust flue gas

$$(E_{\text{Exh}})_{\text{comb}} = \int_{T_0}^{\text{Max.}(T_7,T_8)}\left(1 - \frac{T_0}{T}\right).\text{d}Q = (\dot{m}_g)_s.c_{pg}.\left\{(\text{Max}(T_7,\ T_8) - T_0) - T_0.\ln\left(\frac{\text{Max}(T_7,\ T_8)}{T_0}\right)\right\}. \tag{42}$$

Total exergy lost due to irreversibility

$$(E_{\text{total}})_{\text{comb}} = \sum_1^n (E_n). \tag{43}$$

Exergetic efficiency

$$(\eta_E)_s = \left(\frac{(W_{\text{net}})_{\text{comb}}}{(E_{\text{total}})_{\text{comb}} + (W_{\text{net}})_{\text{comb}}}\right) \times 100. \tag{44}$$

All assumed parameters have been mentioned in Table 1.

3. Technical solution

The combined and topping cycle work net output and efficiencies for the configurations considered have been investigated parametrically by using the first and second laws of thermodynamics. The commercial software EES has been used to obtain a solution for all parametric functions, which have been described by analytical expressions, and then all succeeding parameters and functions have been simulated and implemented.

4. Results and discussion

The variables are the pressure ratio of the topping cycle and the TIT, with the assumption that the pressure dropped through the combustion chamber and H.E. is zero. The

Table 1. Assumed parameters and variables.

Variables			
TIT	900–1000 K	r_p	4–12
Assumed parameters			
η_t	85%	η_c	80%
T_1	300 K	$\varepsilon_1 = \varepsilon_2 = \varepsilon_3$	0.9
$\dot{m}_a$	1 kg s^{-1}	LCV	42 000 kJ kg^{-1} K^{-1}
c_{pa}	1.005 kJ kg^{-1} K^{-1}	γ_a	1.4
c_{pg}	1.14 kJ kg^{-1} K^{-1}	γ_g	1.33

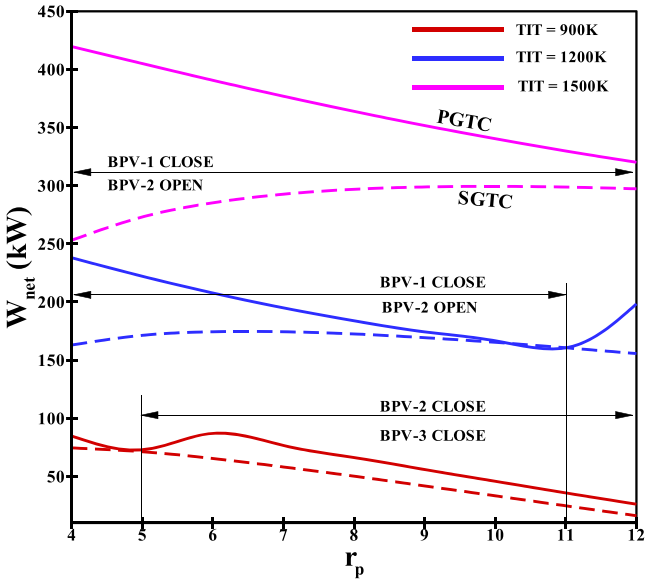

Figure 3. Variation of work net output (W_{net}) w.r.t pressure ratio (r_p) at TIT = 900–1200 K.

exhaust gases from the turbine of the topping cycle release to the environment via a $(H.E.)_1$ if the BPV-2 opens, whereas exhaust gases release to the atmosphere via $(H.E.)_3$, if the BPV-2 close. The compressed air from the bottoming air compressor enters the turbine of the bottoming cycle via (H.E.)2 if the BPV-3 open but via $(H.E.)_3$, if the BPV-3 close, as shown in figure 2.

Variations in work net output (W_{net}) of PGTC and SGTC with compressor pressure ratio (r_p) for different values of TIT were investigated, as shown in figure 3. It is shown in this figure that the network for the topping cycle is less than for the combined cycle, and the network for both the combined and topping cycle increases significantly with TIT, which proves that the TIT significantly affects the work net output of the cycle.

It is also noted that the work net output (W_{net}) of the SGTC and PGTC is almost equal at $r_p = 5$ and $r_p = 11$ for TIT = 900 K and TIT = 1200 K respectively, whereas the work net output of PGTC reaches its maximum valve at $r_p = 6$ for TIT = 900 K and $r_p = 4$ for TIT = 1200 K which is 33% and 46% respectively—more than the SGTC. For TIT = 1500 K, the work net output of the PGTC is much higher than the SGTC throughout the pressure ratio range considered, although the work net output of the PGTC decreases with pressure ratio. The work net output of the PGTC is 65.7% at $r_p = 4$ and 7.6% at $r_p = 12$ more than the SGTC for TIT = 1500 K. It is observed from figure 3 that when BPV-1 is close and BPV-2 is open, that is, the $(H.E.)_1$ and $(H.E.)_2$ is in functional, the Work net output of PGTC decreases, and the reason is that the work net output of the PGTC is the summation of the topping cycle and bottoming cycle. The work net output of the bottoming cycle is the function of the pressure ratio of the bottoming cycle and TIT of the bottoming cycle in equation (34). The pressure ratio of the bottoming cycle is again the function of the TIT of the bottoming cycle in equations (28) and (29). When BPV-1 is closed and BPV-2 is open, the pressure ratio of the bottoming cycle is the function of the TIT of the bottoming cycle (T_{10}), which depends on the temperature of the combustible gases from the combustion chamber (T_4). From equations (18) and (20) it is clear that the temperature of the combustible gases from the combustion chamber (T_4) is the function of the pressure ratio of the topping cycle (r_p). With an increase in pressure ratio, the rate of fuel supply and the inlet temperature of air into the combustion chamber decreases, which results in a decrease in the temperature of the combustible gases from the combustion chamber (T_4). The combined effect of all results shows a decrease in the work net output of the bottoming cycle due to the decrease in the pressure ratio of the bottoming cycle. When the temperature of the combustible gases from the gas turbine of the topping cycle becomes less than or equal to the temperature of compressed air coming from the topping air compressor, then T_4 = TIT and at this stage BPV-1 is opened and BPV-2 is closed. When the BPV-2 is closed, at the same time BPV-3 is also closed, and the combustible product from the gas turbine leaves to the environment through the $(H.E.)_3$ and the compressed air from the bottoming air compressor gains heat from the exhaust gases of the gas turbine from the topping cycle in the $(H.E.)_3$ before it enters the turbine of the bottoming cycle.

In addition, at this stage, the pressure ratio of the bottoming cycle becomes a function of the temperature of the air leaving the $(H.E.)_3$, and due to this reason, the first value of the pressure ratio of the bottoming cycle is higher than the last value of the pressure ratio of bottoming cycle whose value depends on (T_4-TIT). Figure 4 shows the variation in thermal efficiency w.r.t the pressure ratio for the different TITs of the PGTC and SGTC. It is noted that the thermal efficiency significantly increases with an increase in TIT. The maximum

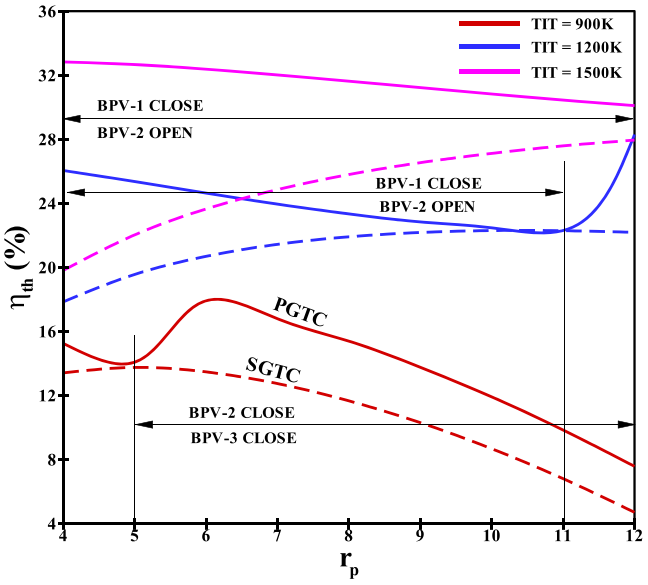

Figure 4. Variation in thermal efficiency (η_{th}) w.r.t pressure ratio (r_p) at TIT = 900–1200 K.

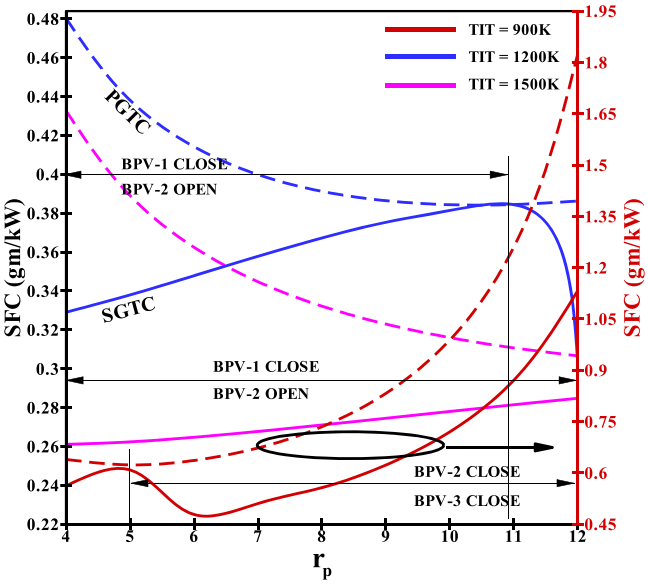

Figure 5. Variation in specific fuel consumption (SFC) w.r.t pressure ratio (r_p) at TIT = 900–1200 K.

thermal efficiency of the PGTC is noted to be $r_p = 6$, $r_p = 12$ and $r_p = 4$ for TIT = 900 K, TIT = 1200 K and TIT = 1500 K respectively, which is 33%, 27.5%, and 65.7% respectively—more than the thermal efficiency of the SGTC at the same corresponding points. It is also noted that the thermal of the PGTC for TIT = 1200 K and the SGTC for TIT = 1500 K at $r_p = 12$ and $r_p = 6.5$ are almost equal, but the work net output of the SGTC for TIT = 1500 K is much more than the work net output of PGTC for TIT = 1200 K at $r_p = 12$ and $r_p = 6.5$ as indicated in figure 3.

SFC is directly proportional to the mass flow rate of fuel and inversely proportional to the work net output of the cycle. Figure 5 shows the variation in SFC for the PGTC and SGTC w.r.t. the pressure ratio of the SGTC for TIT = 900–1200 K. For TIT = 900 K, the SFC is plotted on a secondary *y*-axis, and for TIT = 1200 K and TIT = 1500 K the SFC is plotted on the primary *y*-axis. It can be noted from figure 5 that for TIT = 900 K, the SFC of both the PGTC and SGTC increases with an increase in pressure ratio, although the SFC of the PGTC is less than the SGTC. Figure 2 indicates that the work net output of both the PGTC and SGTC for TIT = 900 K decreases with an increase in pressure ratio, and due to this, the SFC of both cycles increases with an increase in pressure ratio. It is also noted that the SFC of the PGTC for TIT = 900 K from $r_p = 4$ to $r_p = 6$ first increases and reaches its peak at $r_p = 5$ and then decreases to its minimum at $r_p = 6$ because from $r_p = 5$ to $r_p = 6$ work net output increases and beyond $r_p = 6$ work net output continuously decreases till $r_p = 12$. It is observed that the SFC of the SGTC and PGTC decreases with an increase in TIT. For TIT = 1200 K of PGTC, the work net output continuously decreases till $r_p = 11$ as indicated in figure 3, due to which the SFC increases, and from $r_p = 11$ to $r_p = 12$ starts increasing, which results in a decrease in the SFC during this range. For TIT = 1500 K the work net output of PGTC continuously decreases till $r_p = 12$ results in a continuous decrease in the SFC. The SFC of the PGTC, for TIT = 1200 K and SGTC TIT = 1500 K at $r_p = 6.5$ and $r_p = 12$, are equal.

The concept of the combined cycle comes into the picture to utilize the energy loss from the exhaust gases of the gas turbine cycle, so it is very important to do a comparative analysis of the exergy loss from the exhaust gases of the PGTC with the SGTC. Figure 6 shows the comparative analysis of the exergy loss from the exhaust gases of the PGTC and SGTC w.r.t the pressure ratio for TIT = 900–1200 K. It can be observed from figure 6 that exergy loss due to the exhaust gases of the PGTC is much lower than the exergy loss due to the exhaust gases of the SGTC. For TIT = 900 K, 1200 K and 1500 K, the exergy loss from the exhaust gases of the PGTC decreases by 73.1% to 98.7%, 48.6% to 92.8%, and 64.7% to 93.7% respectively. It is noted that the BPV plays a vital role in decreasing the exergy loss of the exhaust gases. In the PGTC for TIT = 900 K the exergy loss from the exhaust gases when BPV-2 and BPV-3 close, decreases by 96.1%, as compared to when BPV-1 close and BPV-2 open, whereas for TIT = 1200 K the exergy loss from the exhaust gases when BPV-1 close and BPV-2 open, decreases by 86.6% compared to when BPV-2 and BPV-3 close.

The total exergy loss of the plant is the summation of the exergy loss of each component of the plant. If the number of components increases, the total exergy loss of the plant also increases accordingly. Figure 7 shows the total exergy loss of the plant w.r.t the pressure ratio for TIT = 900–1200 K. It is noted that the total exergy loss of the PGTC, as well as the SGTC, increases with an increase in the pressure ratio and TIT, but the total exergy loss of the PGTC is much higher than for the SGTC. The total exergy loss of the PGTC for TIT = 900 K, TIT = 1200 K and TIT = 1500 K is 33% to 92.5%, 38.3% to 124%, 77% to 140% higher than the total exergy loss of the SGTC. Exergetic efficiency is defined as the ratio of work net output of the cycle to the sum of the work net output and total exergy loss of the cycle. Figure 8 shows the

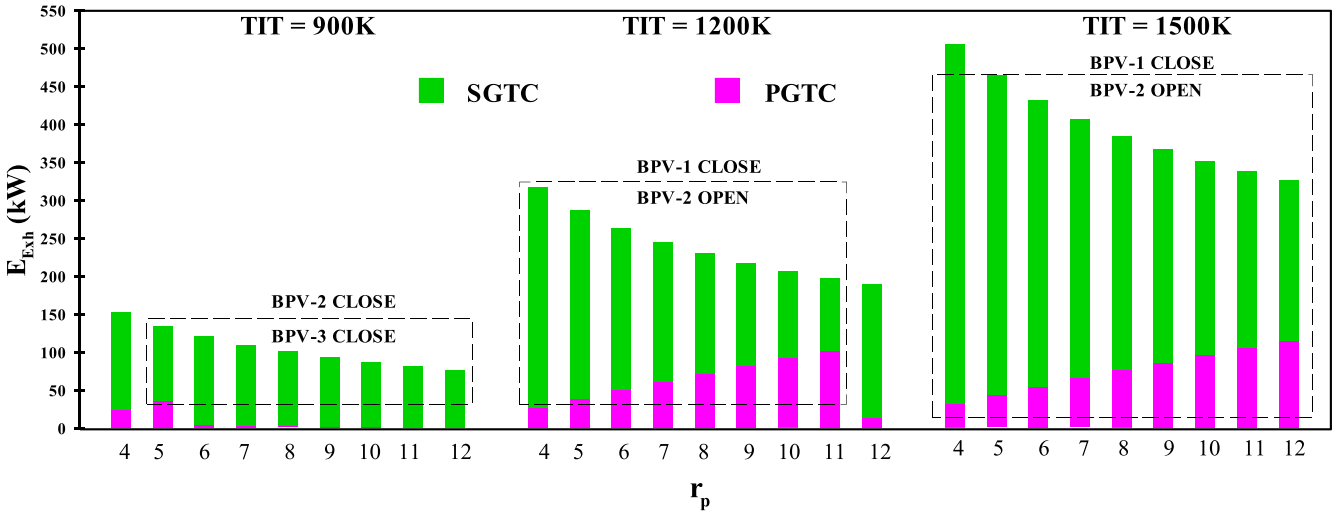

Figure 6. Variation of exergy loss by exhaust gases (E_{Exh}) w.r.t pressure ratio (r_p) at TIT = 900–1200 K.

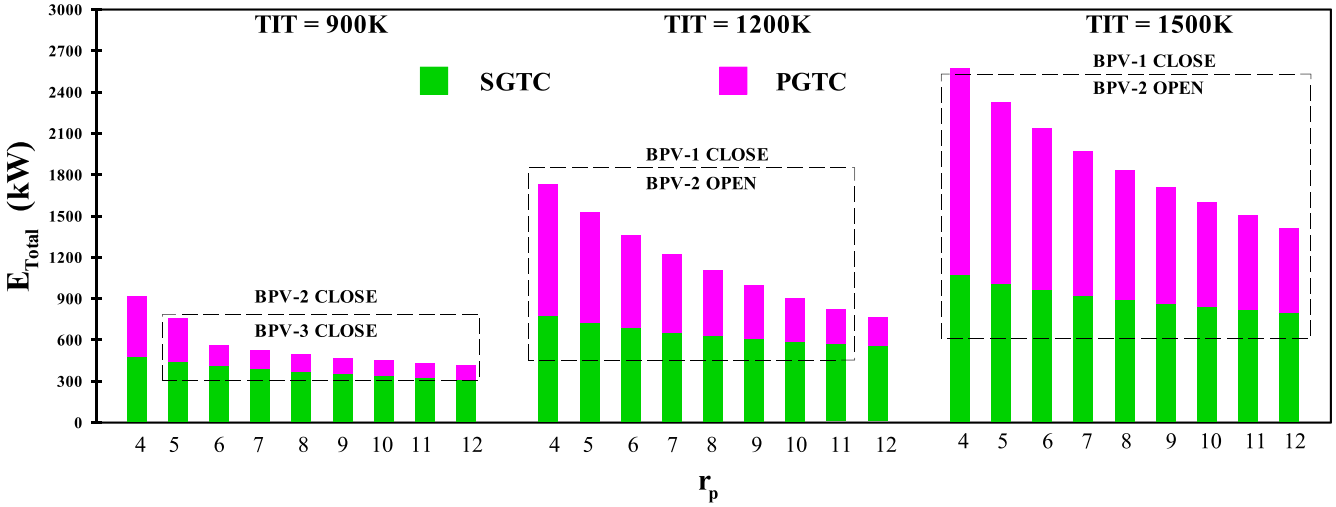

Figure 7. Variation in total exergy loss (E_{Total}) w.r.t pressure ratio (r_p) at TIT =900–1200 K.

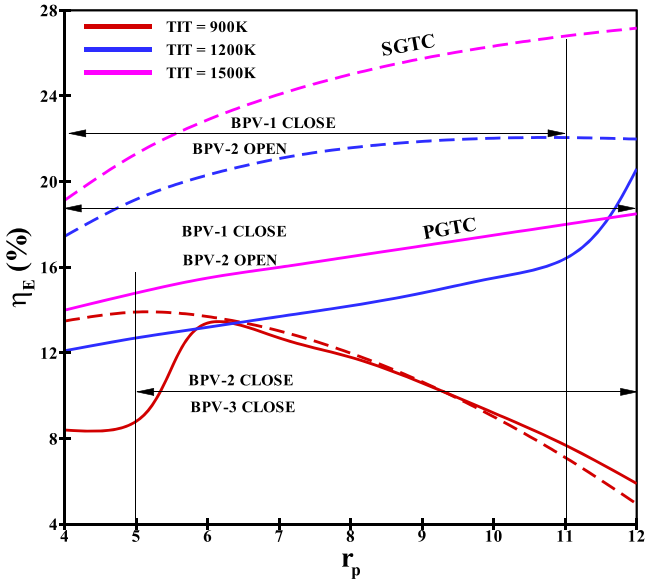

Figure 8. Variation of exergetic efficiency (η_E) w.r.t pressure ratio (r_p) at TIT =900–1200 K.

exergetic efficiency of the PGTC and the SGTC with respect to the pressure ratio for TIT = 900–1200 K. It can be noted from figure 8 that the exergetic efficiency of both the PGTC and SGTC increases with an increase in TIT, but the exergetic efficiency of the SGTC is less than the exergetic efficiency of the PGTC because the total exergy loss of the SGTC is less than the total exergy loss of the PGTC.

5. Conclusion

A parametric investigation for energy and exergy analysis has been carried out for the PGTC and the SGTC using the Ist and IInd law of thermodynamics. H.E.s and bypass control valves were positioned in such a way that the PGTC produce optimum performance in term of energy point of view by varying the pressure ratio and TIT of topping cycle which results in cost of power production and minimizes the exergy loss by the exhaust gases from the topping cycle, that contribute in controlling the global warming. Based on the analyses, as

discussed in section 4, the following conclusions have been drawn:

- TIT plays a significant role in increasing the work net output and thermal efficiency of both the PGTC and SGTC.
- The introduction of BPV and a H.E. in the PGTC increases the energy performance in terms of net output, as well as the thermal efficiency of the cycle, especially for the lower range of TIT.
- The opening and closing of the BPV direct the exhaust gases from the gas turbine of the topping cycle in the PGTC in such a way that maximum heat can be extracted to optimize the combined cycle performance.
- To consider a range of TIT and pressure ratio, the maximum increase in work net output and thermal efficiency of the PGTC as compared to the SGTC is noted as being 65.7% at $r_p = 4$ and TIT = 1500 K.
- The exergy loss from the exhaust gases increases with pressure ratio and TIT for both the PGTC and SGTC.
- The exergy loss from the exhaust gases of the PGTC is much less than the exergy loss from the exhaust gases of the SGTC.
- To consider a range of TIT and pressure ratios, it is noted that the maximum difference in exergy loss from the exhaust gases of the PGTC, as compared to the SGTC, is found for the work net output and thermal efficiency of the PGTC to be at a maximum, that is, at $r_p = 4$ and TIT = 1500 K.

Finally, the present study proves that the proper combination of the BPV and H.E.s is a significant factor in optimizing the cycle performance as observed in PGTC, and to minimize the exergy loss by the exhaust gases.

Acknowledgment

The authors extend their appreciation to the Deanship of Scientific Research at Majmaah University for funding this work under Project Number RGP-2019-16

References

[1] Najafi B, Shirazi A, Aminyavari M, Rinaldi F and Taylor R A 2014 Exergetic, economic and environmental analyses and multi-objective optimization of an SOFC-gas turbine hybrid cycle coupled with an MSF desalination system *Desalination* **334** 46–59

[2] Saghafifar M and Gadalla M 2018 A critical assessment of thermo-economic analyses of different air bottoming cycles for waste heat recovery *Int J Energy Res* **43** 1315–41

[3] Won S, Min H, Seop T and Won D 2018 A novel coolant cooling method for enhancing the performance of the gas turbine combined cycle *Energy* **160** 625–34

[4] Colera M, Soria Á and Ballester J 2019 A numerical scheme for the thermodynamic analysis of gas turbines *Appl. Therm. Eng.* **147** 521–36

[5] Salpingidou C, Tsakmakidou D, Vlahostergios Z, Misirlis D, Flouros M and Yakinthos K 2018 Analysis of turbine blade cooling effect on recuperative gas turbines cycles performance *Energy* **164** 1271–85

[6] Maheshwari M and Singh O 2019 Comparative evaluation of different combined cycle configurations having simple gas turbine, steam turbine and ammonia water turbine *Energy* **168** 1217–36

[7] Ibrahim T k., Kamil M, Awad O I, Rahman M M, Najafi G, Basrawi F, Abd Alla A N and Mamat R 2017 The optimum performance of the combined cycle power plant: a comprehensive review *Renew. Sustain. Energy Rev.* **79** 459–74

[8] Colmenar-santos A, Gómez-camazón D, Rosales-asensio E and Blanes-peiró J 2018 Technological improvements in energetic e ffi ciency and sustainability in existing combined-cycle gas turbine (CCGT) power plants *Appl. Energy* **223** 30–51

[9] Kim M J, Kim J H and Kim T S 2018 The effects of internal leakage on the performance of a micro gas turbine *Appl. Energy* **212** 175–84

[10] Ibrahim T K, Basrawi F, Awad O I, Abdullah A N, Najafi G, Mamat R and Hagos F Y 2017 Thermal performance of gas turbine power plant based on exergy analysis *Appl. Therm. Eng.* **115** 977–85

[11] Salpingidou C, Vlahostergios Z, Misirlis D, Donnerhack S, Flouros M, Goulas A and Yakinthos K 2017 Thermodynamic analysis of recuperative gas turbines and aero engines *Appl. Therm. Eng.* **124** 250–60

[12] Kayadelen H K 2018 Thermoenvironomic evaluation of simple, intercooled, STIG, and ISTIG cycles *Int J Energy Res.* **42** 3780–802

[13] Paepe W D, Montero M, Bram S, Contino F and Parente A 2017 Waste heat recovery optimization in micro gas turbine applications using advanced humidified gas turbine cycle concepts *Appl. Energy* **207** 218–29

[14] Kumari A and Sanjay 2015 Investigation of parameters affecting exergy and emission performance of basic and intercooled gas turbine cycles *Energy* **90** 525–36

[15] Sanjay Sanjay and Prasad B N 2013 Energy and exergy analysis of intercooled combustion-turbine based combined cycle power plant *Energy* **59** 277-284

[16] Selwynraj A I, Iniyan S, Polonsky G, Suganthi L and Kribus A 2015 Exergy analysis and annual exergetic performance evaluation of solar hybrid STIG (steam injected gas turbine) cycle for Indian conditions *Energy* **80** 414–27

[17] Motahar S and Alemrajabi A A 2009 Exergy based performance analysis of a solid oxide fuel cell and steam injected gas turbine hybrid power system *Int. J. Hydrog. Energy* **34** (5) 2396–407

[18] Oyedepo S O, Fagbenle R O, Adefila S S and Alam M M 2015 Performance evaluation of selected gas turbine power plants in nigeria using energy and exergy methods *World Journal of Engineering* **12** 161–76

[19] Leylek Z, Rowlinson G, Anderson W S and Smith N 2013 An investigation into performance modeling of a small gas turbine engine *Proc. ASME Turbo Expo*

[20] Şöhret Y, Ekici S, Altuntaş Ö, Hepbasli A and Karakoç T H 2016 Exergy as a useful tool for the performance assessment of aircraft gas turbine engines: a key review *Prog. Aerosp. Sci.* **83** 57–69

[21] Mishra S and Sanjay Sanjay 2018 Energy and exergy analysis of air-film cooled gas turbine cycle: effect of radiative heat transfer on blade coolant requirement *Appl. Therm. Eng.* **129** 1403–13

[22] Ghazikhani M, Khazaee I and Abdekhodaie E 2014 Exergy analysis of gas turbine with air bottoming cycle *Energy* **72** 599–607

[23] Khaljani M, Khoshbakhti Saray R and Bahlouli K 2015 Comprehensive analysis of energy, exergy and

exergo-economic of cogeneration of heat and power in a combined gas turbine and organic Rankine cycle *Energy Convers. Manage.* **97** 154-165
[24] Elwekeel F N M and Abdala A M M 2016 Effect of mist cooling technique on exergy and energy analysis of steam injected gas turbine cycle *Appl. Therm. Eng.* **98** 298-309
[25] Gadalla M and Saghafifar M 2018 Integration of pulse combustion in air bottoming cycle power plants *Green Energy Technol.* 1 (Cham: Springer) 819–41 Green Energy Technol.
[26] Mehrpooya M, Sayyad S and Zonouz M J 2017 Energy, exergy and sensitivity analyses of a hybrid combined cooling, heating and power (CCHP) plant with molten carbonate fuel cell (MCFC) and Stirling engine *J. Clean. Prod.* **148** 283–94
[27] Khan M N, Tlili I and Khan W A 2017 Thermodynamic optimization of new combined gas/steam power cycles with HRSG and heat exchanger *Arab. J. Sci. Eng.* **42** 4547–58
[28] Alklaibi A M, Khan M N and Khan W A 2016 Thermodynamic analysis of gas turbine with air bottoming cycle *Energy* **107** 603–11
[29] Ghazikhani M, Passandideh-Fard M and Mousavi M 2011 Two new high-performance cycles for gas turbine with air bottoming *Energy* **36** 294–304
[30] Khan M N and Tlili I 2018 New advancement of high performance for a combined cycle power plant: thermodynamic analysis *Case Stud. Therm. Eng.* **12** 166–75
[31] Ayub A, Sheikh N A, Tariq R and Khan M M 2018 Thermodynamic optimization of air bottoming cycle for waste heat recovery *2nd Int. Conf. Energy Syst. Sustain. Dev.*
[32] Yao E, Wang H, Wang L, Xi G and Maréchal F 2017 Multi-objective optimization and exergoeconomic analysis of a combined cooling, heating and power based compressed air energy storage system *Energy Convers. Manage.* **138** 199–209
[33] Park S H, Kim J Y, Yoon M K, Rhim D R and Yeom C S 2018 Thermodynamic and economic investigation of coal-fired power plant combined with various supercritical CO_2 Brayton power cycle *Appl. Therm. Eng.* **130** 611–23
[34] Anvari S, Khalilarya S and Zare V 2019 Power generation enhancement in a biomass-based combined cycle using solar energy: thermodynamic and environmental analysis *Appl. Therm. Eng.* **153** 128–41
[35] Nemati A, Nami H, Ranjbar F and Yari M 2017 A comparative thermodynamic analysis of ORC and Kalina cycles for waste heat recovery: a case study for CGAM cogeneration system *Case Stud. Therm. Eng.* **9** 1–13
[36] Search H, Journals C, Contact A, Iopscience M and Address I P 1995 Power and efficiency in a regenerative gas turbine *Journal of Physics D: Applied Physics* **28** 2020–3
[37] Bianchi M, Pascale A D and Montenegro G 2007 Challenges of power engineering and environment *Proceedings of the International Conference on Power Engineering 2007* (Zhejiang University: Springer-Verlag Berlin Heidelberg)
[38] Wang H, Liu S and Du J 2009 Performance analysis and parametric optimum criteria of a regeneration Bose-Otto engine *Phys. Scr.* **79** 055004
[39] Nishida K, Takagi T and Kinoshita S 2005 Regenerative steam-injection gas-turbine systems *Appl. Energy* **81** 231–46
[40] Carazas F J G, Salazar C H and De Souza G F M 2009 Availability analysis of heat recovery steam generators used in thermal power plants *ECOS 2009—22nd Int. Conf. on Efficiency, Cost, Optimization, Simulation and Environmental Impact of Energy Systems*
[41] Bhargava R K, Bianchi M, De Pascale A, Negri Di Montenegro G and Peretto A 2007 Gas turbine based power cycles - a state-of-the-art review *Challenges on Power Engineering and Environment—Proc. of the Int. Conf. on Power Engineering 2007, ICOPE 2007*
[42] Khaliq A 2009 Exergy analysis of gas turbine trigeneration system for combined production of power heat and refrigeration Systéme de trigénération à turbine à gaz utilisé pour produiré de I' énergie, du chauffage et du froid : analyse de I' exergie *Int. J. Refrig.* **32** 534–45
[43] Khan M N and Tlili I 2018 Performance enhancement of a combined cycle using heat exchanger bypass control: a thermodynamic investigation *J. Clean. Prod.* **192** 443–52
[44] Khan M N and Tlili I 2019 New approach for enhancing the performance of gas turbine cycle: a comparative study *Results Eng.* **2** 100008